1-1-2017

Human Retinal Pigment Epithelial Cells Prefer Proline As A Nutrient And Transport Metabolic Intermediates To The Retinal Side

Jennifer R. Chao

Kaitlen Knight

Yekai Wang

Jianhai Du

JBC Papers in Press. Published on June 14, 2017 as Manuscript M117.788422
The latest version is at http://www.jbc.org/cgi/doi/10.1074/jbc.M117.788422

Human Retinal Pigment Epithelial Cells Prefer Proline as a Nutrient and Transport Metabolic Intermediates to the Retinal Side

Jennifer R. Chao[1*], Kaitlen Knight[1], Abbi L. Engel[1], Connor Jankowski[2], Yekai Wang[3,4], Megan A. Manson[1], Haiwei Gu[5], Danijel Djukovic[5], Daniel Raftery[5], James B. Hurley[1,2], Jianhai Du[3,4*]

[1]Department of Ophthalmology, University of Washington, Seattle, WA 98109

[2]Department of Biochemistry, University of Washington, Seattle, WA 98109

[3]Department of Ophthalmology, West Virginia University, Morgantown, WV 26506

[4]Department of Biochemistry, West Virginia University, Morgantown, WV 26506

[5]Northwest Metabolomics Research Center, Department of Anesthesiology and Pain Medicine, University of Washington, Seattle, WA 98109

Running title: *Metabolite transport in RPE*

*To whom correspondence should be addressed: Jennifer R. Chao, 750 Republican Street, Box 358058, Seattle WA 98109; Phone: (206) 221-0594; Email: jrchao@uw.edu; or Jianhai Du, One Medical Center Dr, PO Box 9193, WVU Eye Institute, Morgantown, WV 26505; Phone: (304)-598-6903; Fax: (304)-598-6928; Email: jianhai.du@wvumedicine.org.

Keywords: Retinal pigment epithelium, Proline, Metabolite transport

ABSTRACT

Metabolite transport is a major function for the retinal pigment epithelium (RPE) to support the neural retina. RPE dysfunction plays a significant role in retinal degenerative diseases. We have used mass spectrometry with ^{13}C tracers to systematically study nutrient consumption and metabolite transport in cultured human fetal RPE. LC MS/MS detected 120 metabolites in the medium from either the apical or basal side. Surprisingly, more proline is consumed than any other nutrient including glucose, taurine, lipids, vitamins, or other amino acids. Besides being oxidized through the Krebs cycle, proline is used to make citrate via reductive carboxylation. Citrate, made either from ^{13}C proline or from ^{13}C glucose, is preferentially exported to the apical side, which is taken up by retina. In conclusion, RPE cells consume multiple nutrients, including glucose and taurine, but prefer proline, and they actively synthesize and export metabolic intermediates to the apical side to nourish the outer retina.

INTRODUCTION

The retinal pigment epithelium (RPE) in the vertebrate eye is a monolayer of polarized pigmented epithelial cells that are situated between the photoreceptors and the choroidal blood supply. The RPE provides critical support for the function of the neural retina. It has many long microvilli at its apical side that wrap around the photoreceptor outer segments. On its basal side the RPE forms convoluted microinfolds that increase its surface area. It transports nutrients and metabolites, recycles retinoids, and engulfs shed outer segment (1,2). Failure of the RPE leads to photoreceptor degeneration in diseases including age-related macular degeneration (AMD), bestrophinopathy and Sorsby fundus dystorphy (3-7).

A major function of the RPE is to transport metabolites between the choroid and retina. Photoreceptors have a high demand for energy and are highly glycolytic; like many cancer cells they metabolize about 90% of the glucose they consume into lactate (8,9). RPE cells directionally transport glucose to the retina and lactate into the blood through highly expressed glucose transporters and monocarboxylate transporters (MCTs) on both the apical and basal membranes (1,10,11). Loss of MCTs causes retinal dysfunction and degeneration (12,13). However, less is known about the transport of other nutrients and metabolites through the RPE.

The RPE requires an active metabolism to support its multiple functions. Either suppression of its mitochondrial metabolism or activation of glycolysis can cause RPE dysfunction to induce an AMD-like phenotype in mouse models (14,15). How the RPE imports nutrients to support its own energy demands is still unclear.

Human fetal RPE (hfRPE) cultures have similar morphological and physiological characteristics to native RPE (16). These cultures have been well characterized as a useful model in evaluating RPE metabolism (17) and RPE diseases, including AMD (18). The RPE cultures used in the experiments conducted in this manuscript are of a similar age in culture as the ones used in previously published studies, including investigations of the cause of AMD.

Mass spectrometry (MS) provides a sensitive, quantitative and high throughput platform to measure metabolites. Transport of metabolites labeled with a stable isotope and biochemical transformations of those metabolites can be monitored. In this report, we use both liquid chromatography (LC) MS/MS and gas chromatography (GC) MS coupled with ^{13}C metabolic flux analysis to investigate how nutrients are consumed and how metabolites are transported through cultured hfRPE cells. Surprisingly, we found that proline is the most preferred fuel for RPE cells. They convert proline into ornithine and mitochondrial intermediates through multiple mitochondrial pathways. We also found that RPE transports metabolic intermediates, including citrate, glutamate, serine, and glycine to its apical side, and that when these metabolites are released from the apical RPE, they can be taken up by the retina. We report here a comprehensive study of nutrient utilization and metabolite transport in RPE. Our findings provide new insights into RPE biochemistry and physiology and its role in the pathogenesis of retinal diseases including AMD.

RESULTS

RPE preferentially consumes proline, glucose and taurine, and it exports metabolic intermediates from both its apical and basal surfaces--To examine how the RPE consumes and metabolizes nutrients, we cultured hfRPE cells on filter membrane inserts (Fig 1A) and quantified metabolites in the RPE culture medium from both the apical and basal chambers at 0 h, 8 h and 24 h after changing the culture to fresh medium (Fig 1B). RPE cells cultured on filter inserts developed the polarity seen in native tissue, including apical microvilli, basal infoldings, and tight junctions as seen by transmission electron microscopy (Supplemental Fig 1). For these experiments, we used a rich RPE medium containing all twenty amino acids, glucose, taurine, pyruvate and other supplements (formulation listed in Supplemental Table 1). We quantified 202 metabolites, covering most major metabolic pathways and detected 110 metabolites in the medium (Supplemental Table 2). Of these metabolites, 53 changed substantially between 0 h and 8 h (fold change >1.3 or <-1.3) (Fig 1B). Surprisingly, more proline was consumed than any of the other metabolites we measured. After 24 h, the amount of proline decreased 15.3-fold on the apical side and 2.1 on the basal side. As expected, RPE also consumed substantial amounts of glucose (-2.5) and taurine (-3.3). Other metabolites decreased by less than -2 fold change. Nutrients in the medium were consumed through multiple pathways including the tricarboxylic acid (TCA), β-oxidation, ketogenesis and pentose phosphate pathway. Intermediates in those pathways accumulated in

the medium at 8 h and 24 h. For example, lactate, 3-hydroxybutyrate, citrate and 1-methyladenosine increased >10 fold at the apical side. (Figure 1B). In general, these intermediates increased earlier and more substantially at the apical side than the basal side, suggesting RPE may actively transport these metabolites. To exclude the influence of filter coating on metabolite transport, we quantified the ratios of metabolites from the two sides from wells with coated inserts without RPE after 24 hour incubation. The metabolites reached equilibrium with ratios between the two sides of less than 1.2. (Supplemental Table 3).

Proline is converted into ornithine and TCA cycle intermediates through both oxidative and reductive pathways--To determine how proline is metabolized, we used U-^{13}C proline to trace its metabolism through known pathways. For example, proline can be reduced to form pyrroline-5-carboxylate (P5C). P5C can be converted into ornithine or glutamate which can feed into the TCA cycle (Fig 2A). To avoid interference from other nutrient sources, we changed the medium into KRB containing only 5 mM glucose and 2 mM U-^{13}C proline. After 1 hour, the intensity of U-^{13}C proline dropped 20% in the medium (Supplemental Fig 2), consistent with our finding that RPE cells prefer proline. Even in the presence of unlabeled glucose, about half the pool of ornithine, glutamate and TCA cycle intermediates were labeled with ^{13}C from ^{13}C proline (Figure 2B). Only ~5% of pyruvate, alanine and lactate become labeled, possibly through malic enzyme activity. Proline can also be hydroxylated to form hydroxyproline. However, we did not detect any ^{13}C hydroxyproline after 1 hour, indicating that free proline may not be hydroxylated into hydroxyproline or that hydroxyproline turnover is slow.

Recently, we reported that reductive carboxylation is a major metabolic pathway in RPE cells (19). When U-^{13}C proline is used to generate citrate by reductive carboxylation, all 5 carbons from citrate are labeled with ^{13}C (M5); if it goes through the classic TCA cycle, one carbon is removed by decarboxylation catalyzed by α-ketoglutarate (αKG) dehydrogenase so the citrate produced is M4 (Fig 2C). We found that M5 citrate/isocitrate is the predominant isotopomer after 1 hour labeling of hfRPE cells with ^{13}C proline. M5 citrate is 2.5 fold more enriched than M4 citrate/isocitrate (Figure 2D). The M3 and M2 isotopomers are derivatives from M5 and M4, respectively after a second round of reactions after citrate lyase. Proline-derived citrate and other intermediates are exported into the medium (Fig 2E). M5 citrate also is the predominant isotopomer in the medium (Fig 2F).

RPE exports proline-derived intermediates preferentially to the apical side. We evaluated the fate of metabolites derived from proline by incubating hfRPE on transwell filters with U-^{13}C proline in DMEM with glucose and 1% FBS on the basal side of the filter (Fig 3A). The enrichment of intermediates with ^{13}C increased from 2 h on both the apical and basal sides and reached its highest point at 24 h (Fig 3B-C). The metabolites at the apical side increased more substantially at 8 h (Fig 3D) but the differences between apical and basal levels were somewhat smaller by 24 h.

RPE exports glucose-derived intermediates preferentially to the apical side--Glucose is considered to be an essential nutrient source for RPE (20). We confirmed this by showing that glucose is consumed significantly in hfRPE culture (Fig 1B). To study how intermediates derived from glucose are exported from RPE cells, we added U-^{13}C glucose at either the apical or basal side with unlabeled glucose on the opposite side and quantified the labeled intermediates from both sides at 8 h, 24 h and 48 h (Fig 4A, 4E). GC MS data showed time-dependent increase of intermediates from glucose metabolism in the medium from both apical and basal sides. Lactate, pyruvate, alanine, serine and glycine are generated from glycolysis, and citrate, malate, glutamate and glutamine are from mitochondrial TCA cycle (Fig 4 and Supplemental Fig 3). When ^{13}C glucose is added to the apical side, the apical intermediates reach steady state by 24 h, while accumulation of most intermediates at the basal side is delayed (Fig

4B-C). The concentration difference of labeled metabolites between apical and basal compartments was highest at 8 h with ~10-fold more on the apical side. (Fig 4D). When ^{13}C glucose is provided on the basal side (Fig 4E), intermediates were labeled more slowly with lower enrichment. The concentration difference also is less obvious for most intermediates, with the exception of glutamine (Fig 4F-H). Serine and glycine labeled with ^{13}C also are exported (Supplemental Fig 3). Since there were high concentrations of unlabeled serine and glycine (0.4 mM) in the DMEM, the apparent enrichment of serine and glycine were diluted to less than 5%. Remarkably, no matter the side to which ^{13}C glucose was added, citrate, glutamate, and glutamine were at higher levels on the apical side than basal side, suggesting that export of these metabolites can supply energy to the outer retina.

Mitochondrial function enhances transport of some metabolic intermediates--We noted that mitochondrial intermediates are exported into the medium. To test the importance of mitochondrial energy metabolism in metabolite transport, we used rotenone to block mitochondrial respiratory complex I in hfRPE cells (Figure 5A). When complex I (NADH dehydrogenase) is inhibited, NADH should accumulate in the mitochondrial matrix. Malate can be exported to the cytoplasm where its reducing power can be transferred through NADH to convert pyruvate to lactate. Pyruvate is drawn away from entering mitochondria and oxaloacetate is drawn out of the matrix as malate. Together these would decrease the matrix concentrations of the substrates for synthesizing citrate (Fig 5A). Consistent with this interpretation, we found that 8 hours of rotenone treatment caused relative increases of lactate and malate and a relative decrease of pyruvate and citrate. We noted that glycine and serine decreased more substantially on the basal side (Fig 5B-C). We also noted that inhibition of mitochondrial metabolism abrogated the apical preference for citrate, malate, glutamate and alanine (Fig 5D). To monitor cell death， we tested the release of LDH from the cells into the medium. There was little evidence of cell death in these experiments (Supplemental Fig 4).

Retina imports metabolites exported by RPE--To determine whether metabolites from the RPE can be imported as nutrients by retina, we co-cultured mouse retina with photoreceptors in contact with the apical side of RPE cells grown on transwell filters. We then added ^{13}C glucose to the basal side (Fig 6A). Retina has a high rate of aerobic glycolysis that metabolizes glucose to lactate. As expected, the retina enhanced accumulation of labeled lactate in both the apical and basal chambers. The retina caused depletion of both citrate and glutamate from the apical medium indicating that they were taken up by the retina. Glutamine accumulated on the apical side but decreased at the basal side. Labeled serine and glycine were depleted only on the basal side (Fig 6B-C). To examine how retina co-culture affected RPE metabolism, we quantified the intracellular metabolites in RPE cells. Only lactate was increased in the RPE cells co-cultured with retina, supporting the idea that RPE imports retina-derived lactate. These results suggest that retina does not significantly impact intracellular glucose metabolism in RPE under these conditions (Fig 6D).

To further examine whether metabolites released into the medium by RPE cells are used by the retina, we compared labeled metabolites in retina from ^{13}C glucose with or without RPE. Strikingly, co-culture with RPE markedly increased lactate, pyruvate, citrate, αKG, alanine, glutamine, serine and glycine (Fig 6E), corroborating our hypothesis that RPE exports intermediates to support the retina (Fig 6F).

DISCUSSION

RPE culture is an excellent *in vitro* model to study RPE function and AMD (17,21). In this study, we used targeted metabolomics to study how the RPE consumes nutrients. Unexpectedly, we found that RPE cells prefer proline as an energy substrate. We also developed a stable

isotope-based approach to trace metabolite transport out of the RPE to either its apical or its basal side, and we showed that metabolites exported from the RPE can support retinal metabolism.

Proline is consumed by RPE cells faster than any other nutrients in the culture medium. Proline is a non-essential amino acid that is not normally included in standard DMEM preparations. However, proline ranging from 10-115 mg/L is typically included in most of the widely used protocols for human RPE culture media (16,21-27). Proline can be provided within the RPE by synthesis either from glutamate by P5C synthase or from ornithine by ornithine aminotransferase (OAT). Deficiency of OAT can cause gyrate atrophy, an inborn error of metabolism characterized by lobular loss of RPE and choroid (28,29). RPE has been identified as the major and most early damaged site in gyrate atrophy (29). Intriguingly, supplementation with proline rescues ornithine cytotoxicity induced by inhibition of OAT in RPE cells (30,31). Under our experimental conditions, glutamate and arginine (the precursor of ornithine) are not significantly used in 24 hours (Figure 1B), indicating that proline in RPE cells is more dependent on exogenous supply.

Proline imported into RPE cells can be catabolized into glutamate for mitochondrial intermediates and into ornithine for urea cycle activity. We found that ^{13}C from proline replaced 50% of the endogenous glutamate, ornithine and mitochondrial intermediates within 1 hour (Fig 2B). Labeled glutamate and ornithine accumulated at 24 hours even in the presence of abundant glutamate, glutamine and arginine in the RPE culture medium (Fig 2B). These results demonstrate that proline is an important nutrient source for RPE metabolism. In addition to being oxidized through the TCA cycle, proline fuels the active reductive carboxylation pathway that we previously reported in RPE cells (19). Reductive carboxylation increases mitochondrial bioenergetics and cellular resistance against oxidative damage. Both mitochondrial dysfunction and oxidative stress are major contributors to the pathogenesis of AMD. Our findings highlight the need to elucidate how proline catabolism contributes to RPE metabolism *in vivo* and how it is influenced in diseased RPE cells.

Proline and its hydroxylated form, hydroxyproline, make up 25% of collagen (32), which is the most abundant protein in extracellular matrix (ECM) and in the collagenous zones of Bruch's membrane (BrM). BrM is located between the RPE and the choroid, and ECM remodeling plays a critical role in the deposition of drusen in BrM in AMD (33). Mutations of ECM metabolism genes have been identified in AMD patients (34). RPE cells control collagen synthesis for BrM (35). Both ^{14}C proline and ^{3}H proline were incorporated in newly synthesized collagen in feline RPE cells and aged primate RPE cells (36,37). In our preparations, RPE cells have abundant free hydroxyproline, however, it is not labeled by ^{13}C proline in 1 hour (Fig 2B). This indicates that the hydroxylation of proline occurs after nascent collagen synthesis (38). It also suggests that the hydroxyproline turnover in collagen synthesis and degradation is a very slow process. Interestingly, one proline transporter, SLC6A20, is one of 154 RPE signature genes that is specifically and highly expressed in human RPE by a comparative study of gene expression from 78 tissues (39). Additional investigations will be required to show how carbons from proline are distributed to various metabolic pathways, how proline is transported and how deprivation of proline in culture impacts RPE differentiation and function.

Besides proline, RPE also consumes substantial amounts of taurine and glucose. Photoreceptors are enriched with taurine and they use glucose for aerobic glycolysis. RPE expresses glucose transporters and taurine transporters, and is enriched with these two nutrients (10,40,41). Taurine supplementation promotes RPE proliferation and suppresses cell death in RPE culture (42,43). As a well-known essential nutrient source, glucose is included in almost all RPE culture protocols. Deprivation of glucose reduces

RPE viability and attempts to rescue glucose-deprived RPE using other energy substrates have not been successful. (20). These reports are consistent with our finding that the RPE needs these two basic nutrients under standard culture conditions.

We found that RPE cells export metabolic intermediates other than lactate and β-hydroxybutyrate into the culture medium. Citrate, glutamate and glutamine are predominantly enriched in the culture medium on the apical side. Little is known about plasma membrane transporters for citrate and glutamine in RPE. Glutamate transporters have been found in cultured RPE cells but their distribution is unknown (44,45). Citrate is a key component of the TCA cycle, an important substrate for lipid biosynthesis, and a chelator for divalent cations like $Ca^{2+,}$ Zn^{2+}, Fe^{2+} and Mg^{2+}(46). Citrate is produced in the mitochondria and exported into the cytosol through the mitochondrial citrate transporter (SLC25a1). Alternatively, citrate can also be synthesized in cytosol from αKG through reductive carboxylation by isocitrate dehydrogenase 1 (47). Three citrate transporters (SLC13A2, SLC13A3 and SLC13A5) are responsible for intracellular citrate transport or for import of citrate from blood (48). The citrate concentration in cerebrospinal fluid is about 0.4 mM (49). ^{13}C NMR spectroscopy has shown that astrocytes, but not neurons, are capable of exporting citrate (46,49). Microvilli from the RPE surround photoreceptors outer segments. Photoreceptor uptake of citrate derived from the RPE might facilitate glycolysis by supplying oxaloacetate to shuttle reducing power into mitochondria, provide acetyl-CoA for fatty acid synthesis, be utilized directly for TCA cycle, and/or regulate divalent cations in the outer segment. Our RPE/retina co-culture experiments showing increased lactate, pyruvate, αKG and glutamine in the mouse retina (Fig 6E) support this hypothesis.

In retina, glutamine is synthesized in glia cells and transported into photoreceptors to generate glutamate. We have reported a neuron-glial metabolism model in which lactate, together with neuron-derived aspartate, is used for glutamine synthesis in Müller cells in the retina (50). Our RPE/retina co-culture experiments revealed increased labeled glutamine in the retina and the apical medium, with no change in RPE cells. Under our culture conditions it appears that lactate produced either by the RPE or by photoreceptors in the retina contributes to glutamine synthesis within Müller cells. Additionally, glutamate is depleted from the apical medium when retina is present, suggesting RPE cells might contribute to the glutamine-glutamate cycle.

Serine and glycine are synthesized from 3-phosphoglycerate, a glycolytic intermediate. Surprisingly, RPE causes a ~7 fold increase in incorporation of ^{13}C from glucose into serine and glycine (Fig 6E). Serine is used for biosynthesis of glycerophospholipids, sphingosine and ceramide. These phospholipids are in high demand for the daily renewal of shed outer segments (51). Glycine is essential for purine biosynthesis. Purines like cGMP, ATP, and hypoxanthine are required for phototransduction (8). Additionally, metabolism of serine and glycine is an important source of NADPH which is needed for anti-oxidative stress and lipid synthesis (52). Recent genome-wide analyses have shown that several key enzymes in the serine and glycine pathways have common variants associated with macular telangiectasia type 2, a neurovascular degenerative retinal disease (53).

In summary, we have shown that proline is a preferred nutrient source for cultured RPE cells. Proline is used to generate mitochondrial intermediates through both oxidative and reductive pathways. We found that RPE cells transport glucose-derived citrate, glutamate, serine and glycine from their apical surface to be used by the retina. These findings reveal how RPE utilizes substrates and provide insights into RPE biochemistry and retinal diseases. It is important to note that we have shown in this study how RPE cells have these preferences when grown in culture. Additional experiments will be required to confirm

that RPE cells in the eye of a live animal have similar preferences for metabolic fuels.

EXPERIMENTAL PROCEDURES

Reagents--Unless otherwise specified, all reagents were obtained from Sigma.

RPE Cell Culture--Human fetal RPE was isolated from fetal tissue (16-18 weeks gestation) as previously reported (19,26) and cultured for 4 weeks to form a confluent, pigmented, monolayer of hexagonal cells. For nutrient transport experiments, RPE cells were passaged and grown on 0.4 μm Transparent PET Membrane inserts (Corning, #353180) pre-coated with matrigel (BD Bioscience) at 1 x 10^5 cells/per insert for 4-6 weeks. The cells were cultured in RPE medium consisting of MEM α (Life Technologies), non-essential amino acids (NEAA, Life Technologies), N1 supplement (Life Technologies), 1% (Vol/Vol) FBS (Atlanta Biologicals), taurine, hydrocortisone and triodo-thyronine (detailed formulation of the medium in Supplemental Table 1). Transepithelial resistance (TER) was measured with a Millicell ERS-2 Epithelial Volt-Ohm Meter (Millipore). The pigmented RPE cells cultured on filter membranes with TER ≥200 Ω•cm^2 were changed into 500 μl of fresh RPE medium or DMEM with 1% FBS and U-^{13}C glucose (Cambridge Isotope Laboratories Inc) or U-^{13}C proline. 20 μl of medium was collected for metabolite analysis.

For the intracellular proline labeling experiments, RPE cells were cultured in pre-coated 6-well plates for 4-6 weeks. Prior to each experiment, the cells were changed into Krebs-Ringer bicarbonate buffer (KRB) (54) containing 5 mM glucose and 2 mM U-^{13}C proline and incubated for 1 hour before collection of medium and cells for metabolite analysis.

Retina and RPE co-culture--RPE cells grown on Millicell-HA filters (Millipore) for 4-6 weeks with TER ≥200 Ω•cm^2 were used for experiments. Isolated mouse retinas were laid on top of the RPE cells with the photoreceptors facing the apical side of the RPE. Four cuts were made to the retina to relieve the curvature and minimal medium was left in the apical chamber to make the retina flat. After one hour, the medium was carefully changed into DMEM containing 1% FBS and 2 mM glutamine with unlabeled glucose at the apical side and U-^{13}C glucose at the basal side.

Sample preparation for metabolite analysis --20 μl of medium was mixed with 80 μl of cold methanol on ice for 15 min to precipitate proteins. The mixture was centrifuged at 13,300 rpm for 15 min at 4°C and the supernatant was lyophilized for analysis by either LC MS/MS or GC MS. For RPE cells, after removing the medium, the cells were quickly rinsed with cold 0.9% NaCl and placed on dry ice to quench metabolism (54). 300 μl of 80% (V/V) methanol was added to each well and cells were scraped, homogenized and spin down at 13,300 rpm at 4°C for 15 min. Supernatant was dried for metabolite analysis and the protein concentrations in the pellet were determined by the BCA assay to normalize the metabolite data (54).

Metabolite analysis by LC MS/MS--The LC MS/MS method was described in detail as previously reported (8,55,56). Briefly, dried metabolites were reconstituted in 200 μl 5 mm ammonium acetate in 95% water, 5% acetonitrile, 0.5% acetic acid and filtered through 0.45-μm PVDF filters. The metabolites were separated by a BEH Amid column (1.7 μm, 2.1 mm X 150 mm, Waters, MA) with an Agilent 1260 LC (Agilent Technologies, Santa Clara, CA) and detected using an AB Sciex QTrap 5500 mass spectrometer (AB Sciex, Toronto, ON, Canada) system. Targeted data acquisition was performed in multiple reaction monitoring (MRM) modes, which are monitored 202 MRM transitions in negative and positive mode listed in Supplemental Table 2. The extracted peaks were integrated using MultiQuant 2.1 software (AB Sciex).

Metabolite analysis by GC MS--All stable isotope labeled metabolites were analyzed by GC MS as reported (8,19,54). Dried samples were derivatized by methoxymine (Sigma) and N-tertbutyldimethylsilyl-N-methyltrifluoroacetamide (TBDMS, Sigma), and analyzed on an Agilent

7890/5975C GC/MS system (Agilent Technologies) using a HP-5MS column (30 m x 0.25 mm x 0.25 μm, Agilent). The peaks were analyzed using Agilent Chemstation software and the measured distribution of mass isotopomers was corrected for natural abundance with IsoCor software. Methylsuccinate was added in each sample as a reference. Enrichment was calculated by dividing the labeled ions by the total ion intensity.

Statistics--Data are expressed as the mean ± SD. The significance of differences between means was determined by unpaired two-tailed t tests or analysis of variance with an appropriate post hoc test. A p value < 0.05 was considered to be significant.

Acknowledgments: We thank Dr. Martin Sadiliek, the director of the University of Washington Chemistry Mass Spectrometry Facility to provide assistance for GC MS analysis.

Conflict of Interest: None declared.

Author contributions: Conceptualization, J.R.C, J.B.H, and J.D; Investigation, J.R.C, K.K., A.L.E., C.J., Y.W., M.A.M., H.G., D.D., D.F., and J.D.; Writing, J.D., J.B.H., and J.R.C.; Funding Acquisition, J.R.C., J.B.H., and J.D; Supervision, J.R.C., J.B.H.; and J.D.

REFERENCES

1. Lehmann, G. L., Benedicto, I., Philp, N. J., and Rodriguez-Boulan, E. (2014) Plasma membrane protein polarity and trafficking in RPE cells: past, present and future. *Experimental eye research* **126**, 5-15

2. Strauss, O. (2005) The retinal pigment epithelium in visual function. *Physiol Rev* **85**, 845-881

3. Sparrow, J. R., Hicks, D., and Hamel, C. P. (2010) The retinal pigment epithelium in health and disease. *Curr Mol Med* **10**, 802-823

4. Ambati, J., and Fowler, B. J. (2012) Mechanisms of age-related macular degeneration. *Neuron* **75**, 26-39

5. Rattner, A., and Nathans, J. (2006) Macular degeneration: recent advances and therapeutic opportunities. *Nat Rev Neurosci* **7**, 860-872

6. Guziewicz, K. E., Sinha, D., Gomez, N. M., Zorych, K., Dutrow, E. V., Dhingra, A., Mullins, R. F., Stone, E. M., Gamm, D. M., Boesze-Battaglia, K., and Aguirre, G. D. (2017) Bestrophinopathy: An RPE-photoreceptor interface disease. *Prog Retin Eye Res*

7. Weber, B. H., Vogt, G., Pruett, R. C., Stohr, H., and Felbor, U. (1994) Mutations in the tissue inhibitor of metalloproteinases-3 (TIMP3) in patients with Sorsby's fundus dystrophy. *Nat Genet* **8**, 352-356

8. Du, J., Rountree, A., Cleghorn, W. M., Contreras, L., Lindsay, K. J., Sadilek, M., Gu, H., Djukovic, D., Raftery, D., Satrustegui, J., Kanow, M., Chan, L., Tsang, S. H., Sweet, I. R., and Hurley, J. B. (2016) Phototransduction Influences Metabolic Flux and Nucleotide Metabolism in Mouse Retina. *J Biol Chem* **291**, 4698-4710

9. Hurley, J. B., Lindsay, K. J., and Du, J. (2015) Glucose, lactate, and shuttling of metabolites in vertebrate retinas. *J Neurosci Res* **93**, 1079-1092

10. Sugasawa, K., Deguchi, J., Okami, T., Yamamoto, A., Omori, K., Uyama, M., and Tashiro, Y. (1994) Immunocytochemical analyses of distributions of Na, K-ATPase and GLUT1, insulin and transferrin receptors in the developing retinal pigment epithelial cells. *Cell Struct Funct* **19**, 21-28

11. Philp, N. J., Wang, D., Yoon, H., and Hjelmeland, L. M. (2003) Polarized expression of monocarboxylate transporters in human retinal pigment epithelium and ARPE-19 cells. *Investigative ophthalmology & visual science* **44**, 1716-1721

12. Philp, N. J., Ochrietor, J. D., Rudoy, C., Muramatsu, T., and Linser, P. J. (2003) Loss of MCT1, MCT3, and MCT4 expression in the retinal pigment epithelium and neural retina of the 5A11/basigin-null mouse. *Investigative ophthalmology & visual science* **44**, 1305-1311

13. Ochrietor, J. D., and Linser, P. J. (2004) 5A11/Basigin gene products are necessary for proper maturation and function of the retina. *Dev Neurosci* **26**, 380-387

14. Zhao, C., Yasumura, D., Li, X., Matthes, M., Lloyd, M., Nielsen, G., Ahern, K., Snyder, M., Bok, D., Dunaief, J. L., LaVail, M. M., and Vollrath, D. (2011) mTOR-mediated dedifferentiation of the retinal pigment epithelium initiates photoreceptor degeneration in mice. *J Clin Invest* **121**, 369-383

15. Kurihara, T., Westenskow, P. D., Gantner, M. L., Usui, Y., Schultz, A., Bravo, S., Aguilar, E., Wittgrove, C., Friedlander, M., Paris, L. P., Chew, E., Siuzdak, G., and Friedlander, M. (2016) Hypoxia-induced metabolic stress in retinal pigment epithelial cells is sufficient to induce photoreceptor degeneration. *Elife* **5**

16. Maminishkis, A., Chen, S., Jalickee, S., Banzon, T., Shi, G., Wang, F. E., Ehalt, T., Hammer, J. A., and Miller, S. S. (2006) Confluent monolayers of cultured human fetal retinal pigment epithelium exhibit morphology and physiology of native tissue. *Investigative ophthalmology & visual science* **47**, 3612-3624

17. Adijanto, J., and Philp, N. J. (2014) Cultured primary human fetal retinal pigment epithelium (hfRPE) as a model for evaluating RPE metabolism. *Experimental eye research* **126**, 77-84

18. Johnson, L. V., Forest, D. L., Banna, C. D., Radeke, C. M., Maloney, M. A., Hu, J., Spencer, C. N., Walker, A. M., Tsie, M. S., Bok, D., Radeke, M. J., and Anderson, D. H. (2011) Cell culture model that mimics drusen formation and triggers complement activation associated with age-related macular degeneration. *Proceedings of the National Academy of Sciences of the United States of America* **108**, 18277-18282

19. Du, J., Yanagida, A., Knight, K., Engel, A. L., Vo, A. H., Jankowski, C., Sadilek, M., Tran, V. T., Manson, M. A., Ramakrishnan, A., Hurley, J. B., and Chao, J. R. (2016) Reductive carboxylation is a major metabolic pathway in the retinal pigment epithelium. *Proceedings of the National Academy of Sciences of the United States of America* **113**, 14710-14715

20. Wood, J. P., Chidlow, G., Graham, M., and Osborne, N. N. (2004) Energy substrate requirements of rat retinal pigmented epithelial cells in culture: relative importance of glucose, amino acids, and monocarboxylates. *Investigative ophthalmology & visual science* **45**, 1272-1280

21. Fronk, A. H., and Vargis, E. (2016) Methods for culturing retinal pigment epithelial cells: a review of current protocols and future recommendations. *J Tissue Eng* **7**, 2041731416650838

22. Maminishkis, A., and Miller, S. S. (2010) Experimental models for study of retinal pigment epithelial physiology and pathophysiology. *J Vis Exp*

23. Hu, J., and Bok, D. (2001) A cell culture medium that supports the differentiation of human retinal pigment epithelium into functionally polarized monolayers. *Mol Vis* **7**, 14-19

24. Gamm, D. M., Melvan, J. N., Shearer, R. L., Pinilla, I., Sabat, G., Svendsen, C. N., and Wright, L. S. (2008) A novel serum-free method for culturing human prenatal retinal pigment epithelial cells. *Investigative ophthalmology & visual science* **49**, 788-799

25. Akrami, H., Soheili, Z. S., Khalooghi, K., Ahmadieh, H., Rezaie-Kanavi, M., Samiei, S., Davari, M., Ghaderi, S., and Sanie-Jahromi, F. (2009) Retinal pigment epithelium culture;a potential source of retinal stem cells. *J Ophthalmic Vis Res* **4**, 134-141

26. Sonoda, S., Spee, C., Barron, E., Ryan, S. J., Kannan, R., and Hinton, D. R. (2009) A protocol for the culture and differentiation of highly polarized human retinal pigment epithelial cells. *Nat Protoc* **4**, 662-673

27. Oka, M. S., Landers, R. A., and Bridges, C. D. (1984) A serum-free defined medium for retinal pigment epithelial cells. *Exp Cell Res* **154**, 537-547

28. O'Donnell, J. J., Sandman, R. P., and Martin, S. R. (1978) Gyrate atrophy of the retina: inborn error of L-ornithin:2-oxoacid aminotransferase. *Science* **200**, 200-201

29. Wang, T., Milam, A. H., Steel, G., and Valle, D. (1996) A mouse model of gyrate atrophy of the choroid and retina. Early retinal pigment epithelium damage and progressive retinal degeneration. *J Clin Invest* **97**, 2753-2762

30. Ueda, M., Masu, Y., Ando, A., Maeda, H., Del Monte, M. A., Uyama, M., and Ito, S. (1998) Prevention of ornithine cytotoxicity by proline in human retinal pigment epithelial cells. *Investigative ophthalmology & visual science* **39**, 820-827

31. Ando, A., Ueda, M., Uyama, M., Masu, Y., Okumura, T., and Ito, S. (2000) Heterogeneity in ornithine cytotoxicity of bovine retinal pigment epithelial cells in primary culture. *Experimental eye research* **70**, 89-96

32. Phang, J. M., Liu, W., and Zabirnyk, O. (2010) Proline metabolism and microenvironmental stress. *Annu Rev Nutr* **30**, 441-463

33. Fernandez-Godino, R., Pierce, E. A., and Garland, D. L. (2016) Extracellular Matrix Alterations and Deposit Formation in AMD. *Adv Exp Med Biol* **854**, 53-58

34. Duvvari, M. R., van de Ven, J. P., Geerlings, M. J., Saksens, N. T., Bakker, B., Henkes, A., Neveling, K., del Rosario, M., Westra, D., van den Heuvel, L. P., Schick, T., Fauser, S., Boon, C. J., Hoyng, C. B., de Jong, E. K., and den Hollander, A. I. (2016) Whole Exome Sequencing in Patients with the Cuticular Drusen Subtype of Age-Related Macular Degeneration. *PLoS One* **11**, e0152047

35. Nita, M., Strzalka-Mrozik, B., Grzybowski, A., Mazurek, U., and Romaniuk, W. (2014) Age-related macular degeneration and changes in the extracellular matrix. *Med Sci Monit* **20**, 1003-1016

36. Li, W., Stramm, L. E., Aguirre, G. D., and Rockey, J. H. (1984) Extracellular matrix production by cat retinal pigment epithelium in vitro: characterization of type IV collagen synthesis. *Experimental eye research* **38**, 291-304

37. Hirata, A., and Feeney-Burns, L. (1992) Autoradiographic studies of aged primate macular retinal pigment epithelium. *Investigative ophthalmology & visual science* **33**, 2079-2090

38. Mitsubuchi, H., Nakamura, K., Matsumoto, S., and Endo, F. (2008) Inborn errors of proline metabolism. *J Nutr* **138**, 2016S-2020S

39. Strunnikova, N. V., Maminishkis, A., Barb, J. J., Wang, F., Zhi, C., Sergeev, Y., Chen, W., Edwards, A. O., Stambolian, D., Abecasis, G., Swaroop, A., Munson, P. J., and Miller, S. S. (2010) Transcriptome analysis and molecular signature of human retinal pigment epithelium. *Human molecular genetics* **19**, 2468-2486

40. Hillenkamp, J., Hussain, A. A., Jackson, T. L., Constable, P. A., Cunningham, J. R., and Marshall, J. (2004) Compartmental analysis of taurine transport to the outer retina in the bovine eye. *Investigative ophthalmology & visual science* **45**, 4099-4105

41. El-Sherbeny, A., Naggar, H., Miyauchi, S., Ola, M. S., Maddox, D. M., Martin, P. M., Ganapathy, V., and Smith, S. B. (2004) Osmoregulation of taurine transporter function and expression in retinal pigment epithelial, ganglion, and muller cells. *Investigative ophthalmology & visual science* **45**, 694-701

42. Gabrielian, K., Wang, H. M., Ogden, T. E., and Ryan, S. J. (1992) In vitro stimulation of retinal pigment epithelium proliferation by taurine. *Curr Eye Res* **11**, 481-487

43. Udawatte, C., Qian, H., Mangini, N. J., Kennedy, B. G., and Ripps, H. (2008) Taurine suppresses the spread of cell death in electrically coupled RPE cells. *Mol Vis* **14**, 1940-1950

44. Maenpaa, H., Gegelashvili, G., and Tahti, H. (2004) Expression of glutamate transporter subtypes in cultured retinal pigment epithelial and retinoblastoma cells. *Curr Eye Res* **28**, 159-165

45. Miyamoto, Y., and Del Monte, M. A. (1994) Na(+)-dependent glutamate transporter in human retinal pigment epithelial cells. *Investigative ophthalmology & visual science* **35**, 3589-3598

46. Westergaard, N., Waagepetersen, H. S., Belhage, B., and Schousboe, A. (2017) Citrate, a Ubiquitous Key Metabolite with Regulatory Function in the CNS. *Neurochem Res*

47. Jiang, L., Boufersaoui, A., Yang, C., Ko, B., Rakheja, D., Guevara, G., Hu, Z., and DeBerardinis, R. J. (2016) Quantitative metabolic flux analysis reveals an unconventional pathway of fatty acid synthesis in cancer cells deficient for the mitochondrial citrate transport protein. *Metab Eng*

48. Pajor, A. M. (2014) Sodium-coupled dicarboxylate and citrate transporters from the SLC13 family. *Pflugers Arch* **466**, 119-130

49. Sonnewald, U., Westergaard, N., Krane, J., Unsgard, G., Petersen, S. B., and Schousboe, A. (1991) First direct demonstration of preferential release of citrate from astrocytes using [13C]NMR spectroscopy of cultured neurons and astrocytes. *Neurosci Lett* **128**, 235-239

50. Lindsay, K. J., Du, J., Sloat, S. R., Contreras, L., Linton, J. D., Turner, S. J., Sadilek, M., Satrustegui, J., and Hurley, J. B. (2014) Pyruvate kinase and aspartate-glutamate carrier distributions reveal key metabolic links between neurons and glia in retina. *Proceedings of the National Academy of Sciences of the United States of America* **111**, 15579-15584

51. Ruggiero, L., and Finnemann, S. C. (2014) Lack of effect of microfilament or microtubule cytoskeleton-disrupting agents on restriction of externalized phosphatidylserine to rod photoreceptor outer segment tips. *Adv Exp Med Biol* **801**, 91-96

52. Ducker, G. S., and Rabinowitz, J. D. (2017) One-Carbon Metabolism in Health and Disease. *Cell Metab* **25**, 27-42

53. Scerri, T. S., Quaglieri, A., Cai, C., Zernant, J., Matsunami, N., Baird, L., Scheppke, L., Bonelli, R., Yannuzzi, L. A., Friedlander, M., Egan, C. A., Fruttiger, M., Leppert, M., Allikmets, R., and Bahlo, M. (2017) Genome-wide analyses identify common variants associated with macular telangiectasia type 2. *Nat Genet*

54. Du, J., Linton, J. D., and Hurley, J. B. (2015) Probing Metabolism in the Intact Retina Using Stable Isotope Tracers. *Methods Enzymol* **561**, 149-170

55. Zhu, J., Djukovic, D., Deng, L., Gu, H., Himmati, F., Chiorean, E. G., and Raftery, D. (2014) Colorectal cancer detection using targeted serum metabolic profiling. *J Proteome Res* **13**, 4120-4130

56. Gu, H., Carroll, P. A., Du, J., Zhu, J., Neto, F. C., Eisenman, R. N., and Raftery, D. (2016) Quantitative Method to Investigate the Balance between Metabolism and Proteome Biomass: Starting from Glycine. *Angew Chem Int Ed Engl* **55**, 15646-15650

FOOTNOTES

This work was supported by NIH Grants EY026030 (to J.D., J.B.H., and J.R.C.), EY06641 (to J.B.H.), EY017863 (to J.B.H.), EY019714 (to J.R.C.) and the Brightfocus Foundation (to J.D. and J.R.C.).

Figure Legends

Figure 1. The nutrient consumption of hfRPE cells from the apical and basal sides. (A) Schematic illustrating hfRPE cultured on transwell filter membranes with 500 µl of RPE medium on each side. (B) Metabolite consumption and generation in RPE. 40 µl of medium was sampled from each side at different time points and metabolites were analyzed by LC MS/MS. Green represents consumed metabolites, and red represents generated metabolites. Data are the average of fold change ± standard deviation over the intensity at 0 h from the apical side with the exception of acetoacetate. Acetoacetate is undetectable at 0 h and its change is represented as fold over intensity at 8 h from the apical side. *P<0.05 vs 0 h control. N=4.

Figure 2. Proline is utilized to generate intermediates through both mitochondrial oxidative and reductive pathways. (A) Schematic for tracing proline metabolism in RPE cells. hfRPE cells were grown in 6 well plates and incubated with U-^{13}C proline (^{13}C carbon in blue) and glucose (^{12}C carbon in black). P5C, 1-Pyrroline-5-carboxylic acid. (B) U-^{13}C proline labeled metabolites in hfRPE. hfRPE cells were incubated with 2mM U-^{13}C proline in the presence of 5mM glucose in KRB for 1 hour. (C) Schematic of mitochondrial oxidative and reductive pathways. Blue is the ^{13}C (labeled) and black is ^{12}C (unlabeled). (D) U-^{13}C proline labeled both oxidative and reductive pathways. M4 citrate/isocitrate derives from the oxidative pathway and M5 citrate/isocitrate derives from the reductive pathway. (E-F) U-^{13}C proline labeled intermediates that are exported into the medium. N=3.

Figure 3. Proline is consumed to generate intermediates in both the apical and basal sides. (A) Schematic illustrating hfRPE cells with U-^{13}C proline added to the basal side. hfRPE was cultured on filter membrane inserts with 500 μl of DMEM containing 5.5 mM glucose and 1% FBS on each side. (B-C) ^{13}C labeled intermediates in the medium from the apical and basal sides. (D) The distribution of ^{13}C proline-labeled intermediates on the apical compared to the basal side. The data are represented as the ratio of the intensity of labeled metabolites from the apical side to that of the basal side. The red line represents an even distribution (ratio=1). *P<0.05 vs 2h control; #P<0.05 vs 8h control. N=3.

Figure 4. Distribution of glucose-derived intermediates in the apical and basal sides. (A, E) Schematic illustrating hfRPE cultured on filter membrane inserts with 500 μl of DMEM containing 2 mM glutamine and 1% FBS on each side. 5.5 mM U-^{13}C glucose was added to either the apical side (A) or the basal side (E), and 5.5mM unlabeled glucose was added to the contralateral side. (B-C, F-G) The ^{13}C labeled intermediates in the medium from the apical and basal side after 8h, 24h and 48h. (D, H) The distribution of ^{13}C glucose-labeled intermediates on the apical compared to the basal side. The data are represented as the ratio of the intensity of labeled metabolites from the apical side to that of the basal side. The red line represents even distribution (ratio=1). *P<0.05 vs 8 h control; #P<0.05 vs 24h control. N=3.

Figure 5. Mitochondrial function is essential for metabolite export. (A) Top: schematic illustrating hfRPE culture on filter membrane inserts with medium containing 5.5 mM glucose and 2mM glutamine in DMEM with 1% FBS in both apical and basal chambers; Bottom: schematic on how inhibition of mitochondrial complex I with Rotenone redistributes the redox from mitochondria to cytosol and impacts metabolite levels. Red denotes increase and green denotes decrease. (B-D) Inhibition of mitochondrial complex I by treatment with Rotenone for 8h. The data are represented as the fold change of metabolite intensity with Rotenone treatment over the untreated control on the apical side (B) and basal side (C). (D) Data are represented as the fold change of metabolite intensity in the basal compartment of untreated controls. *P<0.05 vs Control at the apical or basal side; #P<0.05 vs Rotenone at the apical or basal side. NS, no significance. N=3.

Figure 6. Retina uptake of the metabolites released by RPE. (A) Top: schematic illustrating hfRPE cultured on filter inserts with and without mouse retina overlay. The medium consisted of DMEM with 1% FBS and 2 mM glutamine with unlabeled 5.5 mM glucose on the apical side and 5.5 mM U-^{13}C glucose on the basal side. (B-C) The intensity of labeled metabolites in the apical or basal medium. *P<0.05 vs

RPE cells only. N=3. (D) The intensity of labeled metabolites in the RPE cells. *P<0.05 vs RPE cells only. N=3. (E) The intensity of labeled metabolites in mouse retina. Mouse retina was incubated with U-^{13}C glucose with or without RPE cells. *P<0.05 vs Retina only. N=3. (F) Schematic model of metabolite transport between the RPE and retina.

A

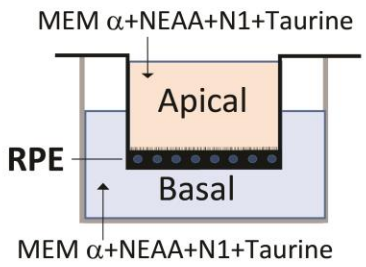

B

	Metabolite	Apical			Basal		
		0h	8h	24h	0h	8h	24h
Amino Acid	Proline	1	-1.4±0.2*	-15.3±2.1*	1.1±0.2	-1.3±0.1*	-2.1±0.4*
	Aspartic Acid	1	-1.3±0.2*	-1.3±0.2*	-1.1±0.1	-1.1±0.2	-1.3±0.3
	Cysteine	1	-1.3±0.3	-2.0±0.3*	1.0±0.3	-1.2±0.2	-1.5±0.3*
	Leucine	1	1.2±0.2	-1.5±0.2*	1.0±0.2	-1.2±0.2	-1.3±0.1*
	Isoleucine	1	-1.2±0.1	-1.6±0.3*	-1.1±0.1	-1.2±0.1	-1.4±0.3*
	Valine	1	-1.1±0.2	-1.3±0.2*	-1.1±0.2	-1.1±0.2	-1.3±0.3
	Glutamine	1	-1.1±0.2	-1.3±0.1*	1.0±0.3	-1.2±0.1	-1.4±0.2*
	Cystine	1	1.0±0.1	-1.4±0.2*	-1.2±0.2	-1.2±0.1	-1.3±0.2*
	Serine	1	-1.2±0.3	-1.3±0.2*	-1.1±0.1	-1.3±0.2*	-1.4±0.3*
	Glycine	1	-1.2±0.2	-1.4±0.2*	-1.1±0.1	-1.2±0.1	-1.5±0.2*
	Ornithine	1	-1.2±0.2	1.6±0.4*	-1.1±0.2	-1.5±0.2*	1.3±0.2*
	Threonine	1	1.0±0.1	-1.2±0.1	1.0±0.2	1.0±0.2	-1.3±0.2*
	Asparagine	1	-1.2±0.2	-1.2±0.2	-1.1±0.3	-1.2±0.2	-1.3±0.2*
	Tyrosine	1	1.0±0.2	-1.1±0.2	-1.1±0.2	-1.1±0.1	-1.3±0.1*
	Lysine	1	1.1±0.3	-1.1±0.1	1.0±0.3	-1.1±0.2	-1.4±0.2*
	Alanine	1	1.0±0.1	1.5±0.2*	-1.1±0.1	1.0±0.2	1.1±0.2
	Glutamate	1	1.0±0.2	1.3±0.3	1.0±0.2	-1.1±0.2	-1.1±0.3
Sugar	Glucose	1	-1.1±0.1	-2.5±0.4*	-1.1±0.1	-1.1±0.1	-1.2±0.1
	Lactose	1	1.0±0.1	-1.3±0.2*	-1.2±0.2	1.0±0.2	-1.1±0.2
Lipid	Arachidonate	1	-1.1±0.1	-1.2±0.3	1.0±0.1	-1.3±0.2*	-1.3±0.2*
	Isovaleric Acid	1	1.1±0.1	-1.4±0.4	1.2±0.2	1.0±0.2	-1.1±0.2
	Margaric Acid	1	-1.1±0.2	-1.3±0.1*	-1.2±0.3	-1.2±0.1	-1.3±0.3
Vitamin	Inositol	1	-1.1±0.1	-1.3±0.2*	-1.1±0.2	-1.1±0.2	-1.1±0.2
	Niacinamide	1	1.0±0.1	-1.3±0.2*	-1.1±0.1	-1.4±0.2*	-1.3±0.2*
	Xanthurenate	1	-1.1±0.2	-1.4±0.3*	1.0±0.1	-1.4±0.2*	-1.3±0.2*
Others	Taurine	1	-1.3±0.3	-3.3±0.7*	-1.1±0.1	-1.5±0.2*	-1.7±0.3*
	Putrescine	1	-1.1±0.2	-1.3±0.2*	1.2±0.2	-1.2±0.2	-1.1±0.2
	Glycerate	1	1.0±0.1	-1.4±0.2*	-1.1±0.1	-1.1±0.2	-1.2±0.2
	Deoxycarnitine	1	1.0±0.1	-1.4±0.3*	1.2±0.3	-1.3±0.3	-1.3±0.3
Glycolysis	G6P/F6P	1	1.9±0.4*	5.0±1.1*	1.3±0.3	2.6±0.5*	4.9±1.8
	Lactate	1	27.7±4.6*	63.9±8.5*	1.1±0.2	11.2±1.5*	42.2±6.8*
TCA Cycle	Citrate	1	4.7±0.4*	14.3±2.3*	-1.1±0.2	4.3±1.1*	6.1±1.7*
	Aconitate	1	1.2±0.2	2.2±0.5*	1.2±0.3	1.2±0.3	1.8±0.6*
	Malate	1	1.4±0.3	2.9±0.6*	-1.1±0.1	1.8±0.4*	2.8±0.5*
	Succinate	1	1.4±0.4	1.7±0.4*	1.1±0.2	1.5±0.2*	2.1±0.7*
	Fumaric Acid	1	1.9±0.6*	4.4±0.9*	-1.2±0.2	1.3±0.3	2.0±0.3*
Ketone bodies	3-Hydroxybutyrate	1	10.2±2.5*	41.6±9.1*	-1.1±0.1	13.5±2.6*	14.5±2.4*
	Acetoacetate	0	1.0±0.3	1.5±0.4*	0.0	1.3±0.4	1.1±0.2
Nucleoside	Guanosine	1	4.1±0.9*	3.8±0.8*	-1.2±0.1	1.9±0.5*	3.3±0.8*
	1-Methyladenosine	1	6.4±1.1*	19.8±4.2*	-1.1±0.2	2.9±0.8*	4.0±1.2*
	Uridine	1	3.1±0.5*	5.8±0.8*	1.1±0.2	1.9±0.5*	5.1±0.6*
	Cytidine	1	1.4±0.2*	3.8±0.6*	-1.2±0.1	2.7±0.5*	2.5±0.5*
	Hypoxanthine	1	1.2±0.3	2.4±0.5*	-1.1±0.2	1.1±0.2	1.8±0.3*
	Inosine	1	1.8±0.4*	1.7±0.4*	-1.2±0.1	1.0±0.1	3.2±0.7*
Others	Acetylcarnitine	1	1.1±0.2	1.7±0.3*	-1.2±0.2	1.1±0.2	1.2±0.1
	Creatine	1	2.0±0.6*	3.2±0.7*	-1.1±0.2	1.2±0.2	1.6±0.4*
	Hydroxyisovalerate	1	3.0±0.8	7.2±1.3*	-1.1±0.1	1.4±0.2*	4.2±
	Betaine	1	1.7±0.4*	6.0±0.7*	-1.2±0.3	1.4±0.3*	3.4±0.8*
	D-Leucic Acid	1	1.0±0.2	4.0±0.9*	-1.2±0.2	1.2±0.2	2.7±0.6*
	Kynurenate	1	2.4±0.5*	3.4±0.7*	1.2±0.1	1.3±0.3	2.6±0.7*
	Shikimic Acid	1	1.5±0.3*	4.3±0.8*	1.1±0.2	1.5±0.2*	2.7±0.6*
	N-AcetylGlycine	1	1.3±0.4	2.1±0.4*	-1.1±0.2	1.3±0.3	1.5±0.2*
	4-Hydroxybutyrate	1	1.3±0.3	1.5±0.2*	-1.2±0.1	1.6±0.3*	1.4±0.2*

< -5.0
-2.1 ~ 5.0
1.3 ~ 2.0
-1.2 ~1.2
-1.3 ~ 2.0
-2.1 ~ 5.0
> 5.0

Figure 1

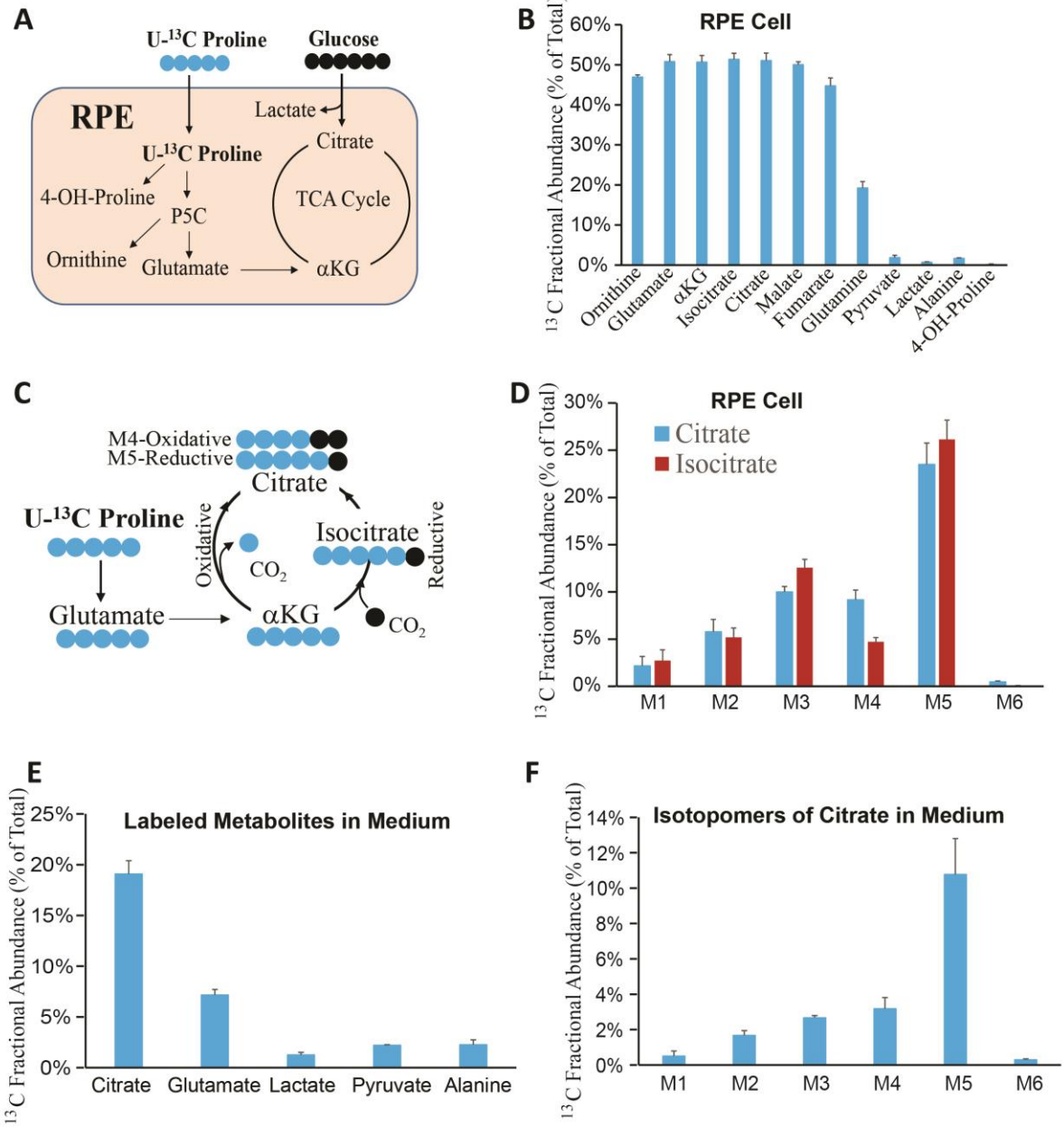
A
U-13C Proline
Glucose
RPE
Lactate
U-13C Proline
Citrate
4-OH-Proline
P5C
TCA Cycle
Ornithine
Glutamate
αKG
B
RPE Cell
13C Fractional Abundance (% of Total)
60%
50%
40%
30%
20%
10%
0%
Ornithine
Glutamate
αKG
Isocitrate
Citrate
Malate
Fumarate
Glutamine
Pyruvate
Lactate
Alanine
4-OH-Proline
C
M4-Oxidative
M5-Reductive
Citrate
U-13C Proline
Oxidative
Isocitrate
Reductive
CO2
Glutamate
αKG
CO2
D
RPE Cell
Citrate
Isocitrate
13C Fractional Abundance (% of Total)
30%
25%
20%
15%
10%
5%
0%
M1
M2
M3
M4
M5
M6
E
Labeled Metabolites in Medium
13C Fractional Abundance (% of Total)
25%
20%
15%
10%
5%
0%
Citrate
Glutamate
Lactate
Pyruvate
Alanine
F
Isotopomers of Citrate in Medium
13C Fractional Abundance (% of Total)
14%
12%
10%
8%
6%
4%
2%
0%
M1
M2
M3
M4
M5
M6

Figure 2

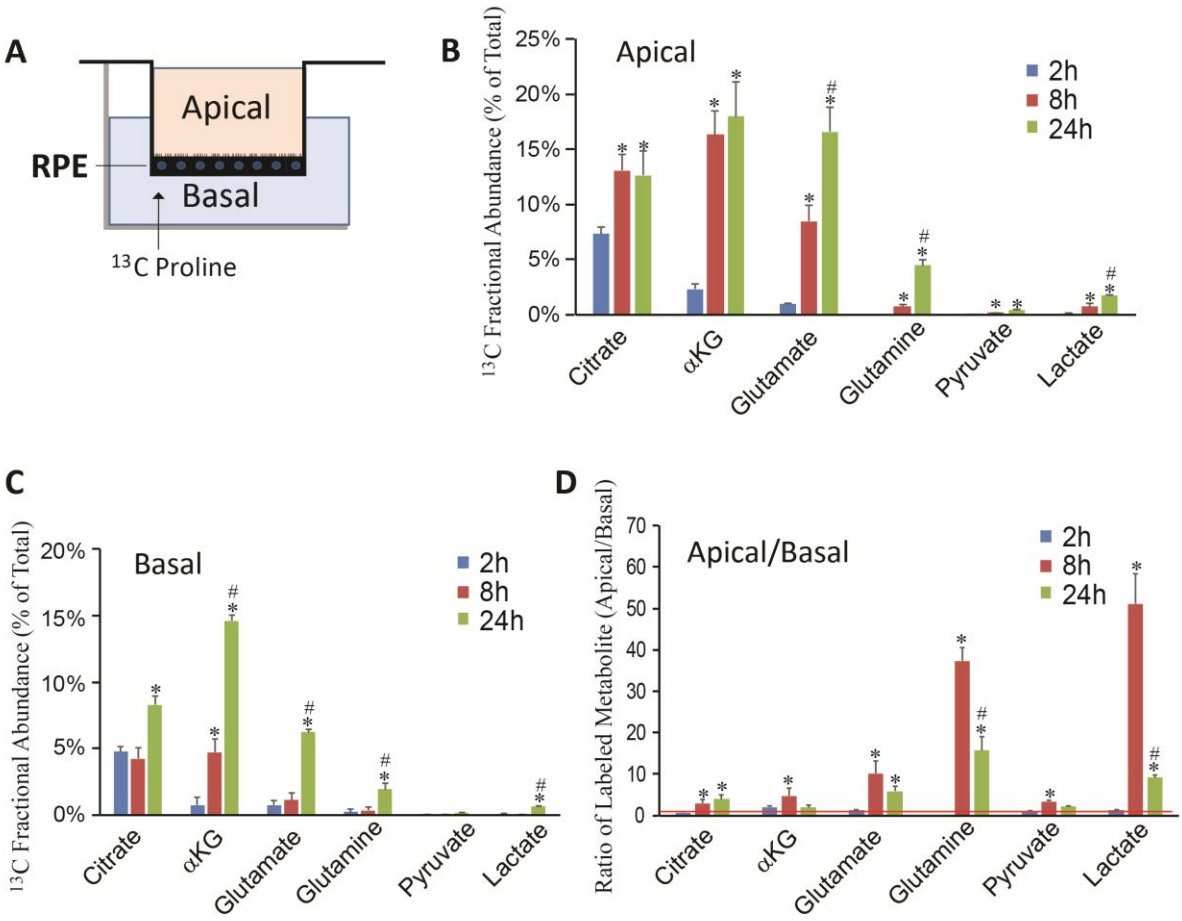
A
Apical
RPE
Basal
13C Proline
B
Apical
2h
8h
24h
13C Fractional Abundance (% of Total)
25%
20%
15%
10%
5%
0%
Citrate
αKG
Glutamate
Glutamine
Pyruvate
Lactate
C
Basal
2h
8h
24h
13C Fractional Abundance (% of Total)
20%
15%
10%
5%
0%
Citrate
αKG
Glutamate
Glutamine
Pyruvate
Lactate
D
Apical/Basal
2h
8h
24h
Ratio of Labeled Metabolite (Apical/Basal)
70
60
50
40
30
20
10
0
Citrate
αKG
Glutamate
Glutamine
Pyruvate
Lactate

Figure 3

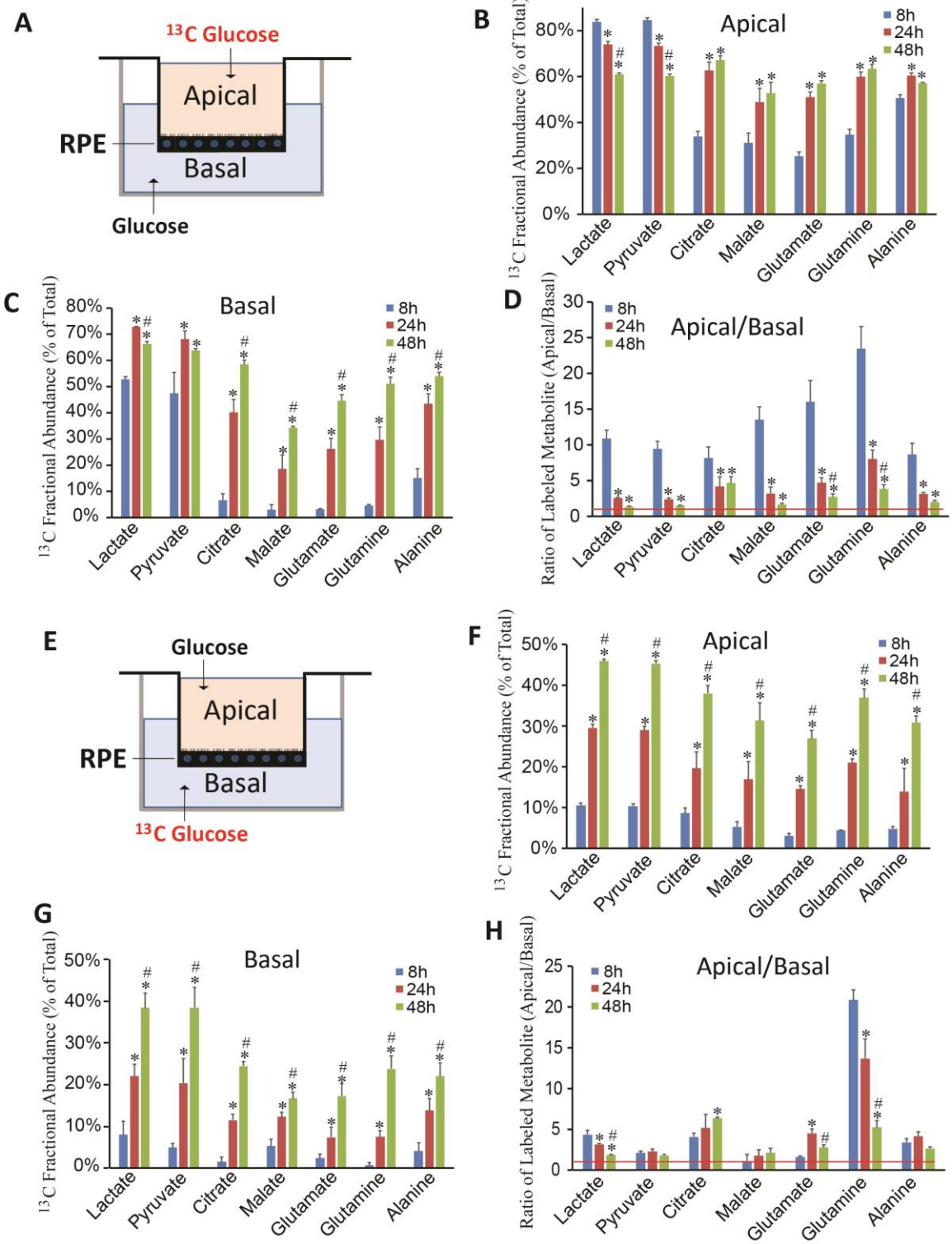
A
13C Glucose
Apical
RPE
Basal
Glucose
B
Apical
8h
24h
48h
13C Fractional Abundance (% of Total)
Lactate
Pyruvate
Citrate
Malate
Glutamate
Glutamine
Alanine
C
Basal
D
Apical/Basal
Ratio of Labeled Metabolite (Apical/Basal)
E
Glucose
Apical
RPE
Basal
13C Glucose
F
Apical
G
Basal
H
Apical/Basal

Figure 4

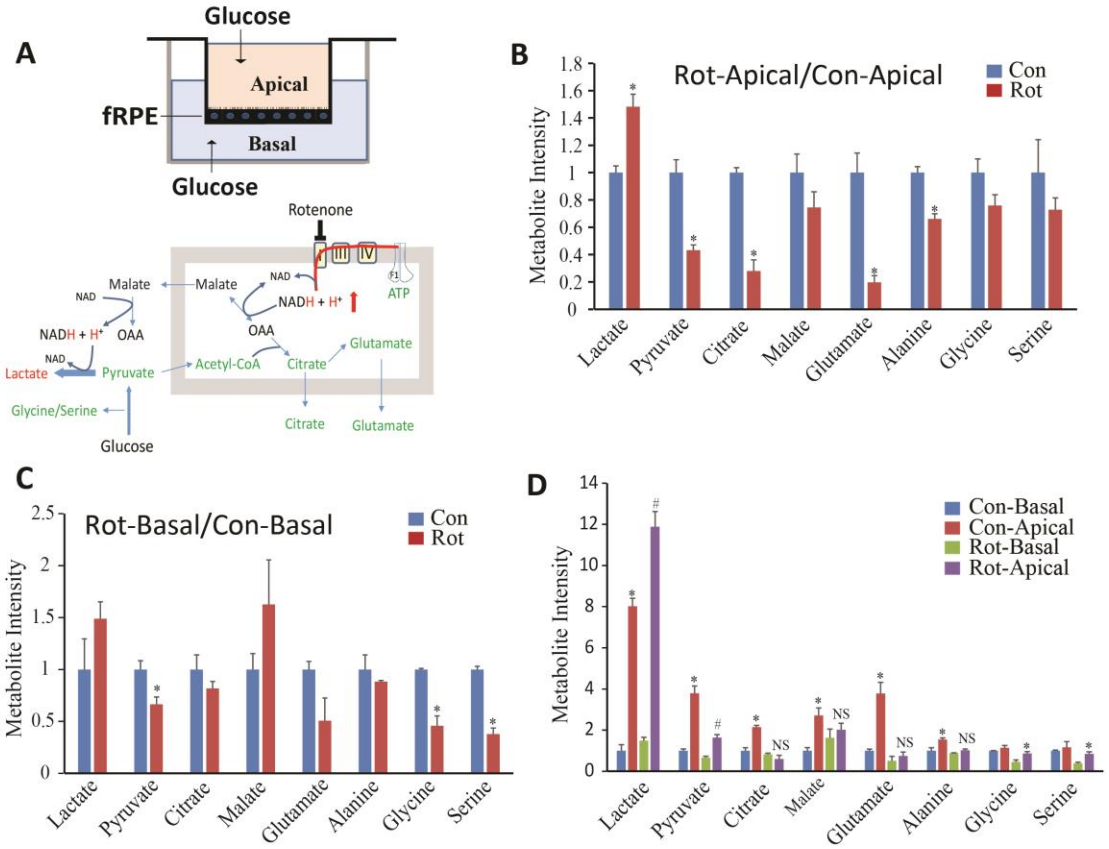
A
Glucose
Apical
fRPE
Basal
Glucose
Rotenone
Malate
NAD
NADH + H+
OAA
Lactate
Pyruvate
Glycine/Serine
Glucose
Acetyl-CoA
Citrate
Glutamate
ATP
B
Rot-Apical/Con-Apical
Con
Rot
Metabolite Intensity
Lactate
Pyruvate
Citrate
Malate
Glutamate
Alanine
Glycine
Serine
C
Rot-Basal/Con-Basal
D
Con-Basal
Con-Apical
Rot-Basal
Rot-Apical
NS

Figure 5

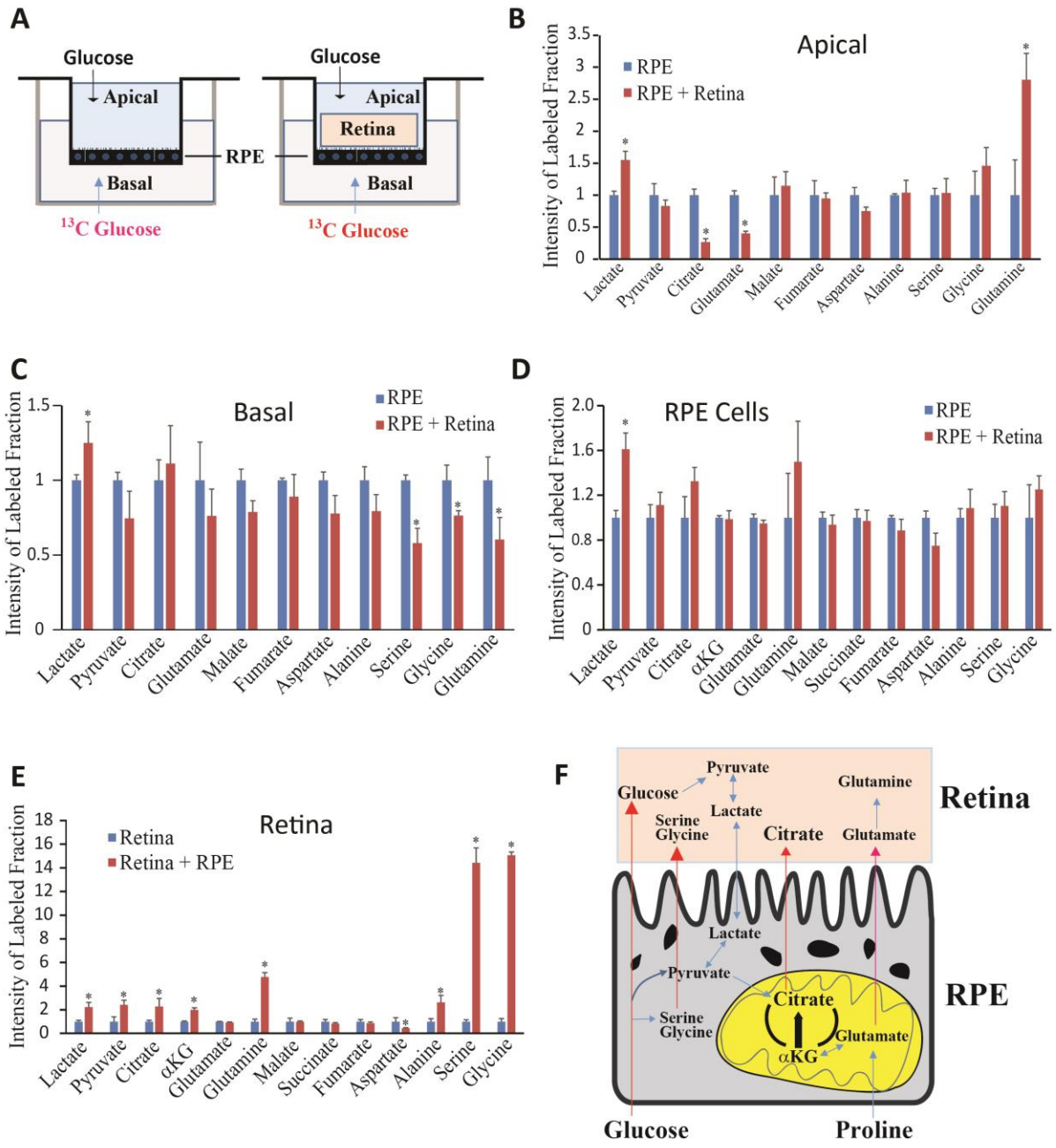
A
Glucose
Apical
RPE
Basal
13C Glucose
Glucose
Apical
Retina
Basal
13C Glucose
B
Apical
RPE
RPE + Retina
Intensity of Labeled Fraction
Lactate
Pyruvate
Citrate
Glutamate
Malate
Fumarate
Aspartate
Alanine
Serine
Glycine
Glutamine
C
Basal
RPE
RPE + Retina
Intensity of Labeled Fraction
Lactate
Pyruvate
Citrate
Glutamate
Malate
Fumarate
Aspartate
Alanine
Serine
Glycine
Glutamine
D
RPE Cells
RPE
RPE + Retina
Intensity of Labeled Fraction
Lactate
Pyruvate
Citrate
αKG
Glutamate
Glutamine
Malate
Succinate
Fumarate
Aspartate
Alanine
Serine
Glycine
E
Retina
Retina
Retina + RPE
Intensity of Labeled Fraction
Lactate
Pyruvate
Citrate
αKG
Glutamate
Glutamine
Malate
Succinate
Fumarate
Aspartate
Alanine
Serine
Glycine
F
Retina
Glucose
Pyruvate
Lactate
Serine
Glycine
Citrate
Glutamine
Glutamate
RPE
Lactate
Pyruvate
Citrate
Serine
Glycine
Glutamate
αKG
Glucose
Proline

Figure 6